Two-dimensional fast generalized Fourier interpolation of seismic records

Mostafa Naghizadeh and Kris Innanen

ABSTRACT

The fast generalized Fourier transform (FGFT) algorithm is extended to two-dimensional (2D) data cases. The 2D FGFT algorithm provides a fast and non-redundant alternative for the simultaneous time-frequency and space-wavenumber analysis of the data with time-space dependencies. The transform decomposes the data based on the local slope information, and therefore making it possible to extract weight function based on dominant dips from the alias-free low frequencies. By projecting the extracted weight function to the alias-contaminated high frequencies and utilizing a least-squares fitting algorithm, a beyond-alias interpolation method is accomplished. Synthetic and real data examples are provided to examine the performance of the proposed interpolation method.

INTRODUCTION

Reconstruction and interpolation of seismic records have become critical elements of the data processing chain. They represent a post-acquisition remedy for the shortcomings of seismic surveys, by synthesizing regular and dense spatial sampling. This in turn makes possible the use of many wave equation demultiple and migration methods, and substantially improves the resolution of seismic images formed from the data. How the interpolation problem is managed in any given situation is in large part determined by the distribution of the spatial samples of the original data before interpolation. This distribution can be regular or irregular. Irregularly sampled data also come in two types, either involving randomly missing samples on a regular grid, or being purely irregular.

Methods such as the anti-leakage Fourier transform (Xu et al., 2005) and band- limited Fourier reconstruction (Duijndam et al., 1999), which utilize discrete Fourier transforms (DFTs) rather than fast Fourier transforms (FFTs), are appropriate for purely irregular data, but are computationally demanding. Alternatively, by deploying an appropriate binning strategy, purely irregular data can be transformed into data with randomly missing samples on a regular grid. This exposes the data to the suite of more computationally efficient FFT based methods, such as minimum weighted norm interpolation (Liu and Sacchi, 2004), and projection onto convex sets (Abma and Kabir, 2005), and non-Fourier methods such as singular value decomposition (Trickett, 2003), singular spectrum analysis (Oropeza and Sacchi, 2011), and Cadzow interpolation (Cadzow and Ogino, 1981; Trickett and Burroughs, 2009). In this paper we will use the term irregular sampling to mean random missing samples on a uniform grid, and consider only this type of irregularity.

Another determining factor in seismic data interpolation is the spatial aliasing problem caused by coarse sampling. A common approach for de-aliasing seismic records is to utilize alias-free low frequencies to remove aliasing from high frequencies. Spitz (1991) and Porsani (1999) used prediction filters in the *f-x* domain to de- alias regularly sampled seismic data. Naghizadeh and Sacchi (2007) developed a multi-step autoregressive (MSAR)

reconstruction method in order to generalize Spitz (1991) to the case of irregularly sampled data. Following the same rationale, Guitton and Claerbout (2010) used the Pyramid transform for beyond-alias interpolation of seismic records; Gulunay (2003), Curry (2009), and Naghizadeh (2010) have introduced *f-k* domain variants of the Spitz *f-x* idea. Recently, Vassallo et al. (2010), Ozbek et al. (2010), and Ozdemir et al. (2010) have introduced a new approach for the removal of aliasing from multi- component seismic data, which does not depend on extrapolating from low frequencies. In their framework, gradient information recorded in one component of the seismic data is used to regularize beyond alias.

All of the methods discussed above have in common the assumption that the seismic data are composed of linear events in the time-space (*t-x*) domain, which have a simple, or sparse, representation in the Fourier domain (Sacchi et al., 1998; Naghizadeh and Sacchi, 2010b). If a given seismic data set contains curved or otherwise more complicated events, as they often do, then a windowing procedure is typically employed, with windows designed such that within them events are locally linear, or stationary. One alternative to spatial windowing, introduced by Naghizadeh and Sacchi (2009) involves estimation of adaptive local prediction filters in the *f-x* domain. Recently, Naghizadeh and Innanen (2011) utilized a new transform referred to as the fast generalized Fourier transform (Brown et al., 2010) to interpolate curved, or nonstationary, seismic events in the *f-x* domain. The FGFT is a fast, non-redundant tool for analysis of nonstationary signals, whose implementation has very low computational cost and memory storage.

In this paper we extend our exposition of the technique of FGFT interpolation, and we extend the method to the two-dimensional (2D) case. We begin by developing the theoretical basis of 2D FGFT interpolation and its practical implementation in the *f-k* domain. We focus on the features of the 2D algorithm which lead to the extraction of the weight function by which low frequencies are used to move beyond alias. Finally, we examine the performance of the method on synthetic and field data examples.

THEORY

S-transform

The S-transform for a one-dimensional (1D) time signal is defined as (Stockwell et al., 1996)

$$S(\tau, f) = \int_{-\infty}^{\infty} g(t) \frac{|f|}{\sqrt{2\pi}} e^{-\frac{(\tau-t)^2 f^2}{2}} e^{-i2\pi f t} dt, \tag{1}$$

where τ and f represent the time and frequency coordinates, respectively. The width of the Gaussian window $\frac{|f|}{\sqrt{2\pi}} e^{-\frac{(\tau-t)^2 f^2}{2}}$ decreases with increasing frequency. This results in finer frequency resolution for low frequencies and finer time resolution for high frequencies. If the window function is set to unity, equation 1 reverts to the ordinary Fourier transform.

One can generalize the S-transform to a two-dimensional (2D) time-space dependent

signal using

$$S(\tau,\chi,f,k)=\int_{-\infty}^{\infty} g(t,x)\frac{|f||k|}{2\pi}e^{-(\frac{(\tau-t)^2f^2+(\chi-x)^2k^2}{2})}e^{-i2\pi(ft+kx)}dtdx, \tag{2}$$

where τ and χ are the time and space and f and k are the frequency and wavenumber coordinates, respectively. The term $\frac{|f||k|}{2\pi}e^{-(\frac{(\tau-t)^2f^2+(\chi-x)^2k^2}{2})}$ is a 2D Gaussian window which depends on time and space lags as well as frequency and wavenumber. The size of the Gaussian window decreases with increasing frequency and wavenumber. This results in finer frequency/wavenumber resolution for low frequencies/wavenumbers and finer time/space resolution for high frequencies/wavenumbers.

The implementation of S-transform in the time domain would require a cumbersome set of operations including windowing and convolution. However, the equivalence of S-transform in the frequency domain is composed of a simple combination of operations such as shifting, windowing and inverse Fourier transform. Brown et al. (2010) further utilized the simple form of S-transform in the frequency domain to introduce a fast and non-redundant S-transform which they named fast generalized Fourier transform (FGFT). In 1D signals the FGFT entails dividing the frequency domain of data into smaller window sizes and performing inverse Fourier transform in each individual window. The size of windows in the frequency domain varies based on the center frequency, by choosing smaller windows for low frequencies and larger windows for higher frequencies. For a more detailed explanation on 1D FGFT see Brown et al. (2010) and Naghizadeh and Sacchi (2010a).

2D fast generalized Fourier transform

The FGFT algorithm introduced by Brown et al. (2010) can be easily generalized to the 2D *t-x* data. Following the same rationale of applying windowed IFFT in the frequency domain, the *f-k* domain of data can be divided into small rectangular windows shown in Figure 1a. By applying 2D inverse Fourier transforms inside each of these rectangles one can obtain the 2D FGFT domain representation of the data. The gray color rectangles, in Figure 1a represent the portion of FGFT domain which will be used for developing a beyond-alias seismic interpolation method. For interpolation purposes, the directional properties of each window in the 2D FGFT domain are very important. This is due to the fact that after applying inverse 2D Fourier transform in each window of Figure 1a, each window will then contain a distinct range of slopes. It should be mentioned that 2D FGFT windowing of the *f-k* domain is very similar to that of standard wavelet transform. However, in 2D FGFT the whole operation is carried out in the Fourier domain without necessity of up-sampling or down-sampling of data in the *t-x* domain needed to perform 2D wavelet transform. This difference in implementation results in a global phase for 2D FGFT algorithm and a local phase for 2D wavelet transform (Brown et al., 2010) .

One can also perform a directional decomposition of the *f-k* domain using curvelet transform (Candes et al., 2005) shown in Figure 1b. The U-shaped areas of curvelet windows in the *f-k* domain are depicting the scales of the curvelet transform (odd scales are shown by gray areas and even scales are shown by white in Figure 1b). In addition, each

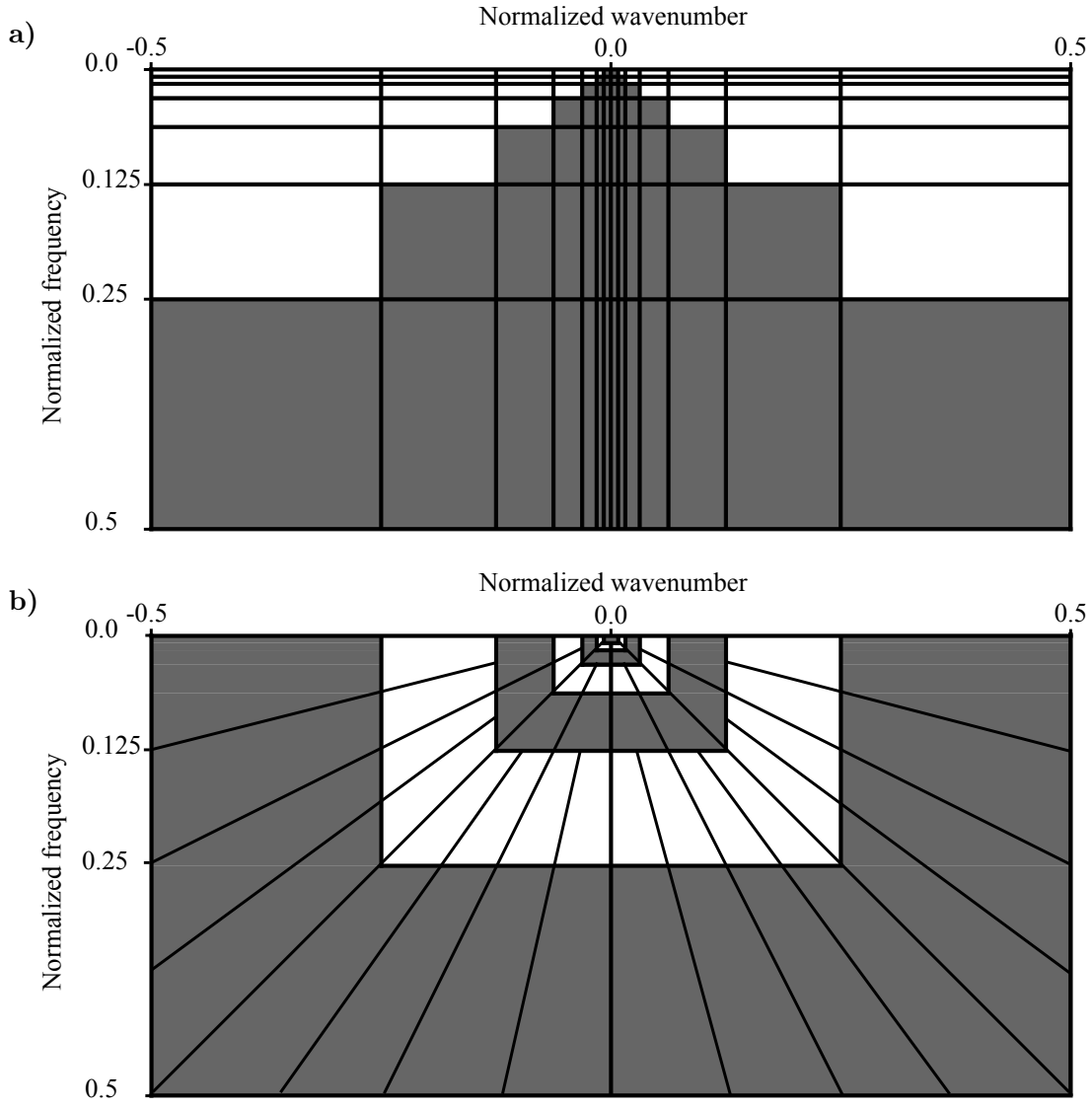

FIG. 1. a) The structure of *f-k* domain tiles used for 2D FGFT transform. b) The structure of *f-k* domain tiles used in curvelet transform.

scale is divided into smaller directional windows. While Curvelet transform has better direction-based windowing of the *f-k* domain its windows do not have rectangular shapes (Naghizadeh and Sacchi, 2010a). Therefore, performing inverse 2D Fourier transforms for each window of curvelet transform requires extra adjustments and operations which can result in a redundant transform domain. Notice that the directional decompositions in the curvelet domain are better resolved than 2D FGFT. Naghizadeh and Sacchi (2010b) used the directional properties of the curvelet domain for beyond-alias interpolation of seismic records. In this article we will adapt a similar strategy for the interpolation of seismic data using 2D FGFT coefficients.

We use an example of simple synthetic seismic data to explain the implementation of 2D FGFT algorithm. Figure 2a shows a synthetic seismic section composed of three hyperbolic events. Figure 2b shows the *f-k* spectra of data in Figure 2a. We have overlaid the *f-k*

domain windowing scheme of 2D FGFT algorithm on the *f-k* spectra of the data. Figure 2c shows the 2D FGFT domain of data which is obtained by applying inverse Fourier transform for each small window in Figure 2b. It is interesting that this set of simple operation has been able to effectively decompose the data into distinctive slope range for given frequency ranges. We will utilize this feature of 2D FGFT algorithm for beyond-alias interpolation of seismic records.

2D FGFT interpolation of seismic data

Let's represent the regularly sampled 2D seismic data $\mathbf{d}_{(N_t,N_x)}$, where N_t and N_x show the number of temporal and spatial samples of data, respectively. For simplicity of notation we drop the time dependency of the variables since we are only interested in interpolation spatial direction. This means that a specific missing spatial sample in the data will be equal to N_t missing samples from all data set corresponding to the given trace at that spatial location. Now, the data can be represented as $\mathbf{d} = (\mathbf{d_1}^T, \mathbf{d_2}^T, \ldots, \mathbf{d_{N_x}}^T)^T$. Next we assume that we only have M out of N spatial samples (traces) available, and that the remaining $N - M$ traces are missing. We represent the available samples as $\mathbf{d}_{\text{obs}}$. The desired signal $\mathbf{d}$ and observed samples $\mathbf{d}_{\text{obs}}$ are related by a sampling matrix $\mathbf{T}$ (Naghizadeh and Innanen, 2011), through:

$$\mathbf{d}_{\text{obs}} = \mathbf{T}\mathbf{d}\,. \tag{3}$$

Let's explain the structure of sampling matrix $\mathbf{T}$ using a simple example. Assume that the desired signal $\mathbf{d}$ has 5 traces with N_t time samples, but only 3, say $\{\mathbf{d_1}, \mathbf{d_3}, \mathbf{d_4}\}$, are available. Equation 3 can be written as

$$\begin{pmatrix} \mathbf{d_1} \\ \mathbf{d_3} \\ \mathbf{d_4} \end{pmatrix} = \begin{pmatrix} \mathbf{I} & \mathbf{0} & \mathbf{0} & \mathbf{0} & \mathbf{0} \\ \mathbf{0} & \mathbf{0} & \mathbf{I} & \mathbf{0} & \mathbf{0} \\ \mathbf{0} & \mathbf{0} & \mathbf{0} & \mathbf{I} & \mathbf{0} \end{pmatrix} \begin{pmatrix} \mathbf{d_1} \\ \mathbf{d_2} \\ \mathbf{d_3} \\ \mathbf{d_4} \\ \mathbf{d_5} \end{pmatrix}, \tag{4}$$

Where $\mathbf{I}$ and $\mathbf{0}$ are $N_t \times N_t$ sized identity and zero matrices, respectively. The transpose of the sampling matrix, $\mathbf{T}^T$, correctly places the available samples in the output and puts zeros in the samples corresponding to missing data.

The interpolation problem is under-determined and therefore we require some prior information to obtain a stable and regularized solution. To provide this, let us consider the 2D FGFT coefficients $\mathbf{g}$ of the desired, fully sampled signal. These must be related to $\mathbf{d}$ by

$$\mathbf{g} = \mathbf{G}\,\mathbf{d}\,, \tag{5}$$

where $\mathbf{G}$ represents the forward 2D FGFT operator. The adjoint 2D FGFT operator $\mathbf{G}^T$ can furthermore be used to express the desired interpolated data $\mathbf{m}$ in terms of $\mathbf{g}$ as follows

$$\mathbf{d} \approx \mathbf{G}^T\,\mathbf{W}\,\mathbf{g}\,, \tag{6}$$

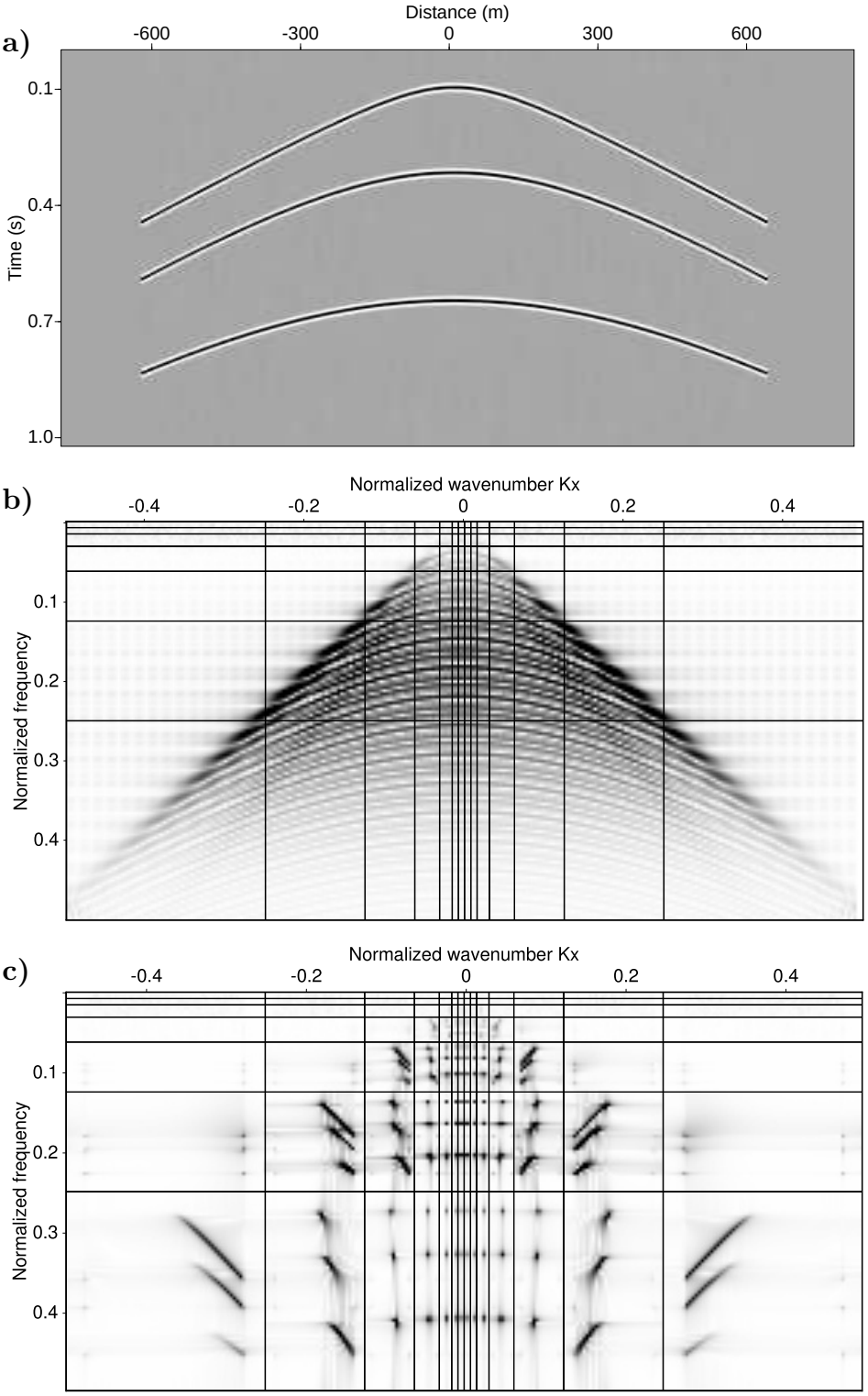

FIG. 2. a) Synthetic seismic record in the *t-x* domain. b) The *f-k* spectra of data. c) 2D FGFT representation of data.

where we have introduced a diagonal weight function $\mathbf{W}$ that preserves a subset of 2D FGFT coefficients. Inserting equation 6 into 3 yields

$$\mathbf{d}_{\text{obs}} \approx \mathbf{T}\mathbf{G}^T\,\mathbf{W}\,\mathbf{g}\,. \tag{7}$$

Let us assume for the moment that the operator $\mathbf{W}$ is known. The system of equations in equation 7 is under-determined (Menke, 1989) and therefore, it admits an infinite number of solutions. A stable and unique solution can be found by minimizing the following cost function (Tikhonov and Goncharsky, 1987)

$$J \;=\; ||\mathbf{d}_{\text{obs}} - \mathbf{T}\,\mathbf{G}^T\mathbf{W}\mathbf{g}||_2^2 + \mu^2||\mathbf{g}||_2^2\,, \tag{8}$$

where μ is the trade-off parameter. We minimize the cost function J using the method of conjugate gradients (Hestenes and Stiefel, 1952). The conjugate gradients method does not require the explicit knowledge of $\mathbf{G}$ in matrix form. It requires the action of operators $\mathbf{G}^T$ and $\mathbf{G}$ on a vector in the coefficient and data spaces, respectively (Claerbout, 1992). The goal of the proposed algorithm is to find the coefficients $\hat{\mathbf{g}}$ that minimize J, and use them to reconstruct the data via the adjoint 2D FGFT operator $\hat{\mathbf{d}} = \mathbf{G}^T\hat{\mathbf{g}}$.

Derivation of the weight function W

In order to create a stable interpolation scheme using the 2D FGFT algorithm some preparatory operations on seismic data are needed. First, for aliased data (wrap-around energy around the frequency axis) a regular scheme of zero trace interlacing is required. The number of zero traces interlaced between each pair of available traces is determined by the severity of aliased energy. We define the natural number $n_a \geq 1$ as the alias severity factor (ASF). The normalized frequency on which aliasing starts, f_a, and the ASF are related by

$$0.5^{n_a+1} \leq f_a < 0.5^{n_a}, \tag{9}$$

or in other words

$$n_a = -(\lfloor log_2(f_a) \rfloor - 1), \qquad 0 < f_a < 0.5, \tag{10}$$

where $\lfloor . \rfloor$ means truncation to the nearest smaller integer number. The number of zero traces, n_{ztr}, needed to be interlaced between original grid of data is given by

$$n_{ztr} = 2^{n_a} - 1. \tag{11}$$

The interlaced zero traces are treated as missing samples by the sampling function $\mathbf{T}$. Notice that interlacing zero traces allows us to extract correct slope information from low frequencies in order to interpolate the high frequencies.

Next we divide the frequency axis of the 2D FGFT domain into two groups: alias-free and alias-contaminated ranges. The weight function, $\mathbf{W}$, for alias-free 2D FGFT coeffi-

cients is derived by

$$\begin{array}{l}\text{For } i = n_a, n_a+1, n_a+2, \ldots \\ \quad f \in [0.5^{i+2}, 0.5^{i+1}) \\ \quad \text{If} \quad k \in [-(0.5^{i+1}), 0.5^{i+1}] \\ \qquad \mathbf{W}(f,k) = \begin{cases} 0 & \mathbf{g}(f,k) < \lambda_i \\ 1 & \mathbf{g}(f,k) \geq \lambda_i \end{cases}, \\ \quad \text{Else} \\ \qquad \mathbf{W}(f,k) = 0 \\ \quad \text{End} \\ \text{End}\end{array} \tag{12}$$

where λ_i represents the threshold values for each frequency range. Notice that 2D FGFT coefficients residing in the non-evanescent part of *f-k* spectra are set to zero. The weight function, $\mathbf{W}$, works as mask function to preserve high amplitude 2D FGFT coefficients and annihilate the low amplitude ones.

For alias contaminated frequency ranges the weight function is computed from the weight function of alias-free frequency ranges via

$$\begin{array}{l}\text{For } i = na, na-1, \ldots, 1 \\ \quad f_h \in [0.5^{i+1}, 0.5^{i}) \\ \quad k_h \in [-(0.5^{i}), 0.5^{i}] \\ \quad f_l \in [0.5^{i+2}, 0.5^{i+1}) \\ \quad k_l \in [-(0.5^{i+1}), 0.5^{i+1}] \\ \quad \mathbf{W}(f_h, k_h) = \mathbf{\Omega}(\mathbf{W}(f_l, k_l)), \\ \text{End}\end{array} \tag{13}$$

where $\mathbf{\Omega}$ is a simple nearest neighbor interpolation operator which doubles the width and length of the input matrix. The procedure for computing weight function can be easily explained using Figure 1a. Assuming $n_a = 1$, for the normalized frequencies smaller than 0.25, the white-colored 2D FGFT tiles are set to zero and the gray-colored 2D FGFT tiles are thresholded based on the predefined threshold value for each frequency range. Now for the normalized frequency range $[0.25, 0.5)$ the weight function is obtained by doubling the size of the weight function in the range $f \in [0.125, 0.25)$ and $k \in [-0.25, 0.25]$.

EXAMPLES

Synthetic seismic data

We begin by applying 2D FGFT interpolation on a synthetic seismic data set composed of 3 hyperbolic events. Figure 3a shows the original synthetic seismic section. Next, we set to zero every other trace of the original seismic section to obtain the data with missing traces in Figure 3b. Figure 3c shows the output of 2D FGFT interpolation. The difference between original and interpolated data is shown in Figure 3d. Figure 3e-h show the *f-k* spectra of the data in Figures 3a-d, respectively. The 2D FGFT interpolation was successful in removing a significant amount of aliased energy from the missing data. Notice that the main leftover energies in the *f-k* spectra of the difference (Figure 3h) reside in the corners of the 2D FGFT tiles. This is the price paid for having non-redundant and in-place transform. These artifacts can be removed effectively if we use overlapped tiles in the *f-k* domain.

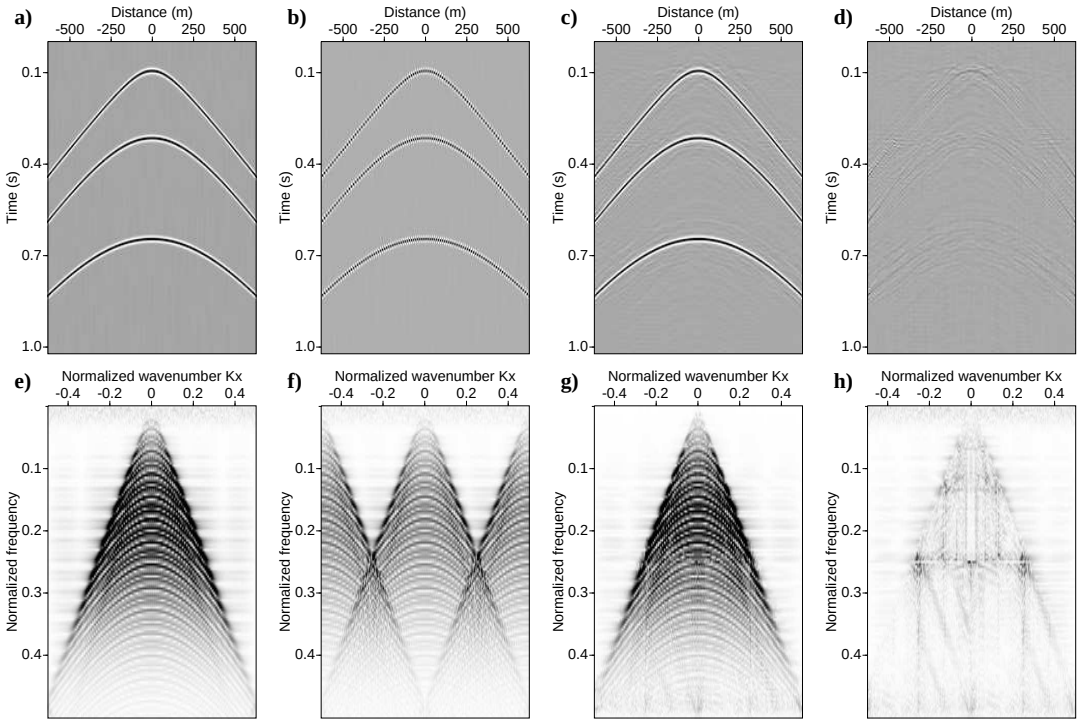

FIG. 3. a) Original synthetic seismic data. b) Data after replacing every other traceswith zero traces. c) Interpolated data using 2D FGFT method. d) The difference between a and c. e-h) are the *f-k* spectra of a-d, respectively.

Figure 4a shows the 2D FGFT representation of the data with missing traces in Figure 3b. It is obvious that alias energy in the normalized frequency range $[0.25, 0.5)$ appears as false slope information in the 2D FGFT domain. Figure 4b shows the weight function computed using the expressions 12 and 13. Notice that for the normalized frequencies below 0.25 only band-limiting and thresholding operations have applied. For the normalized frequencies $[0.25, 0.5)$ the mask function has been upscaled from the normalized frequencies $[0.125, 0.25)$. This operation guarantees preservation of correct slope information and removal of false slopes from the aliased part of the *f-k* spectra. Figure 4c shows the 2D FGFT representation of the interpolated data. It is obvious that aliased energy has been removed after interpolation.

Figure 5a shows the data in Figure 3a after randomly eliminating 40% of the traces. Figure 3b shows the interpolated data using 2D FGFT interpolation method. Figure 3c shows the difference between original and interpolated data. Figures 3d-f represent the *f-k* spectra of the data in Figures 3a-c, respectively. The 2D FGFT interpolation has successfully removed the leaked energy in the *f-k* domain of data with randomly missing traces.

Figure 6a shows the 2D FGFT representation of the data in Figure 5b. It is clear that random sampling has created low amplitude false slope information in the 2D FGFT domain. Figure 6b depicts the mask function computed using Equations 12 and 13. In order to effectively remove the spectral leakage of random sampling operator it is useful to update the mask function using few external iterations after each least-squares fitting of the

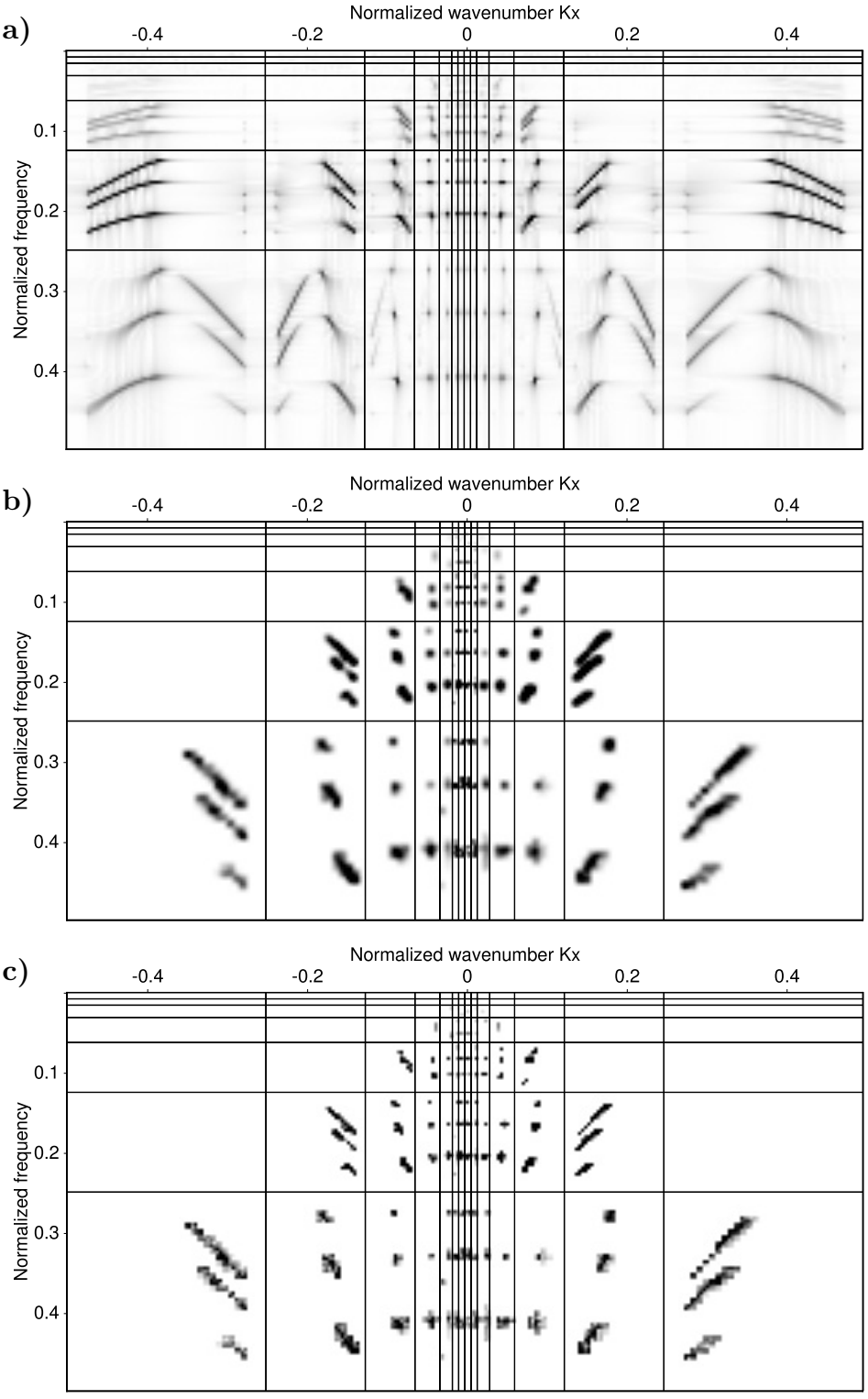

FIG. 4. a) 2D FGFT representation of data with missing traces in Figure 3a. b) Mask function built using Equations 12 and 13. c) 2D FGFT representation of interpolated data in Figure 3c.

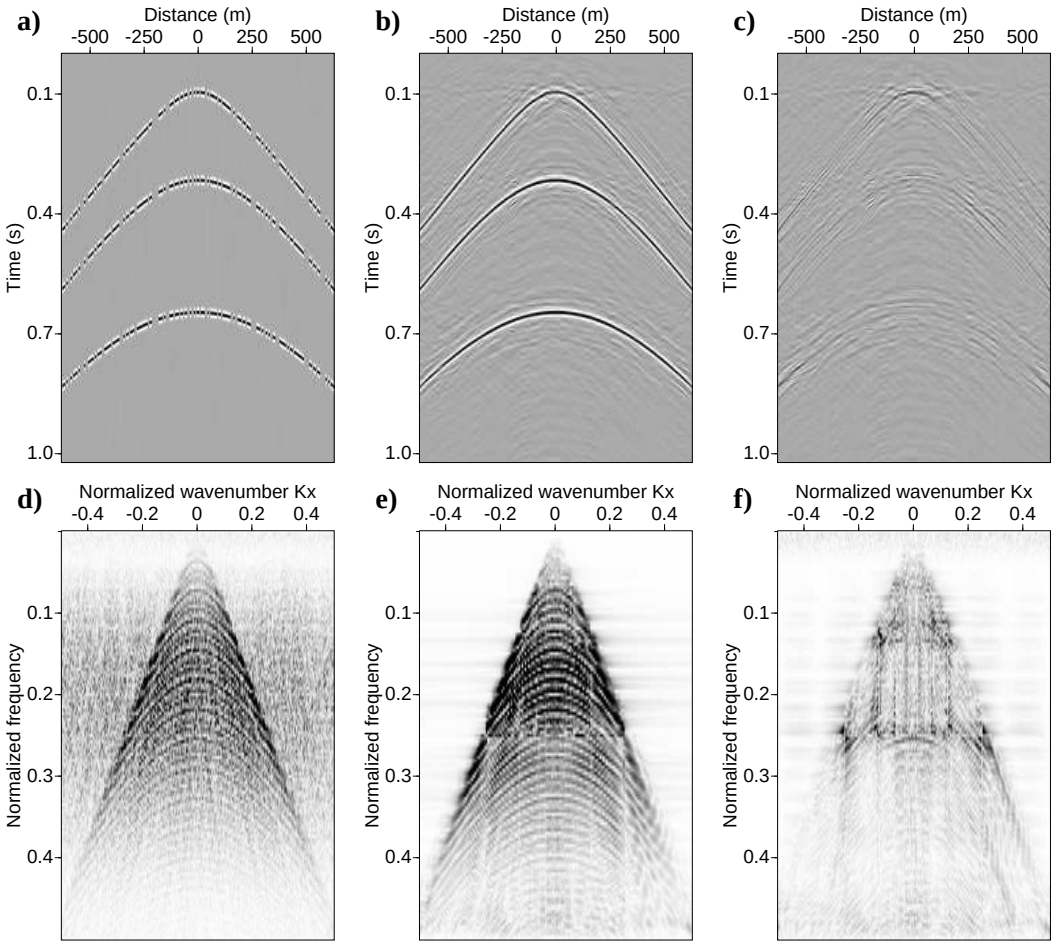

FIG. 5. a) Seismic data in Figure 3a after randomly eliminating 40% of the traces. b) Interpolated data using 2D FGFT method. d) The difference between 3a and b. d-f) are the *f-k* spectra of a-c, respectively.

data. Figure 6c shows the 2D FGFT representation of the interpolated data. It is clear that most of the leaked energy is eliminated by the proper estimation of the weight function.

Field data example

Figure 7a shows a real shot gather from the Gulf of Mexico data set. The data were interpolated using 2D FGFT interpolation and the output is shown in Figure 7b. Figures 7c and 7d show the *f-k* spectra of the data in Figures 7a and 7b, respectively. It is clear that the interpolated data no longer contain aliased energy. Notice that in Figure 7c the aliased wrap-around energy starts at the normalized frequency $f_a = 0.15$. This means the ASF for this data is equal to $n_a = 2$, therefore, we need to add $n_{ztr} = 3$ zero traces between each available pair of traces to prepare data for the 2D FGFT interpolation method.Figures 8a and 8b show a small window of the original and interpolated data, respectively. The 2D FGFT interpolation has been successful in preserving AVO and curvature characters of seismic events.

Figure 9a shows the original shot gather after adding 3 zero traces between each pair of available traces. Figure 9b shows the *f-k* spectra of data in Figure 9a. Interlacing 3 zero traces in the original data in the *t-x* domain produced 3 replicas of the original spectra of the data. Figure 10a shows the 2D FGFT representation of the data in Figure 9a. Figure 10b shows the 2D FGFT representation of the interpolated data after extracting proper weight function using equations 12 and 13 and applying it to interpolated data. It is clear that the weight function has successfully removed most of the aliased energy.

DISCUSSION

The 2D FGFT interpolation is an attempt to develop a fast and non-redundant interpolation technique for spatially non-stationary seismic records. It decomposes the curved seismic records based on their local slope and their frequency and wavenumber number content. This slope based data decomposition permits the design of simple weight (mask) function which can be deployed effectively to remove the aliased energy. The implementation of 2D FGFT is straightforward as it only requires tiling the *f-k* domain with various sizes of rectangular windows and performing Inverse Fourier transforms in each localized *f-k* window. The computations of the 2D FGFT is an in-place operations and therefore there is no need for extra memory storage spaces. The 2D FGFT algorithm, in nature, is similar to the standard 2D discrete wavelet transform. The main difference between these two approachs is in the way they handle the phase of the data Gibson et al. (2006). The 2D FGFT algorithm has a global phase reference while the 2D wavelet transform retains local phase references (Brown et al., 2010). This also means that the same strategy used in this article for interpolation of seismic records can be easily adapted for the 2D wavelet transform as well.

For an optimal implementation of 2D FGFT algorithm one needs to smooth the corners of the tiles of 2D FGFT segmentation of the *f-k* spectra using Gaussian style windows. This help to avoid the artifacts caused by the Gibbs phenomena due to the sharp windowing of data. Another alternative remedy is to zero-pad the sides of the data in the *t-x* domain. This ensures that some of the side effects caused by sharp windowing will appear in the zero-

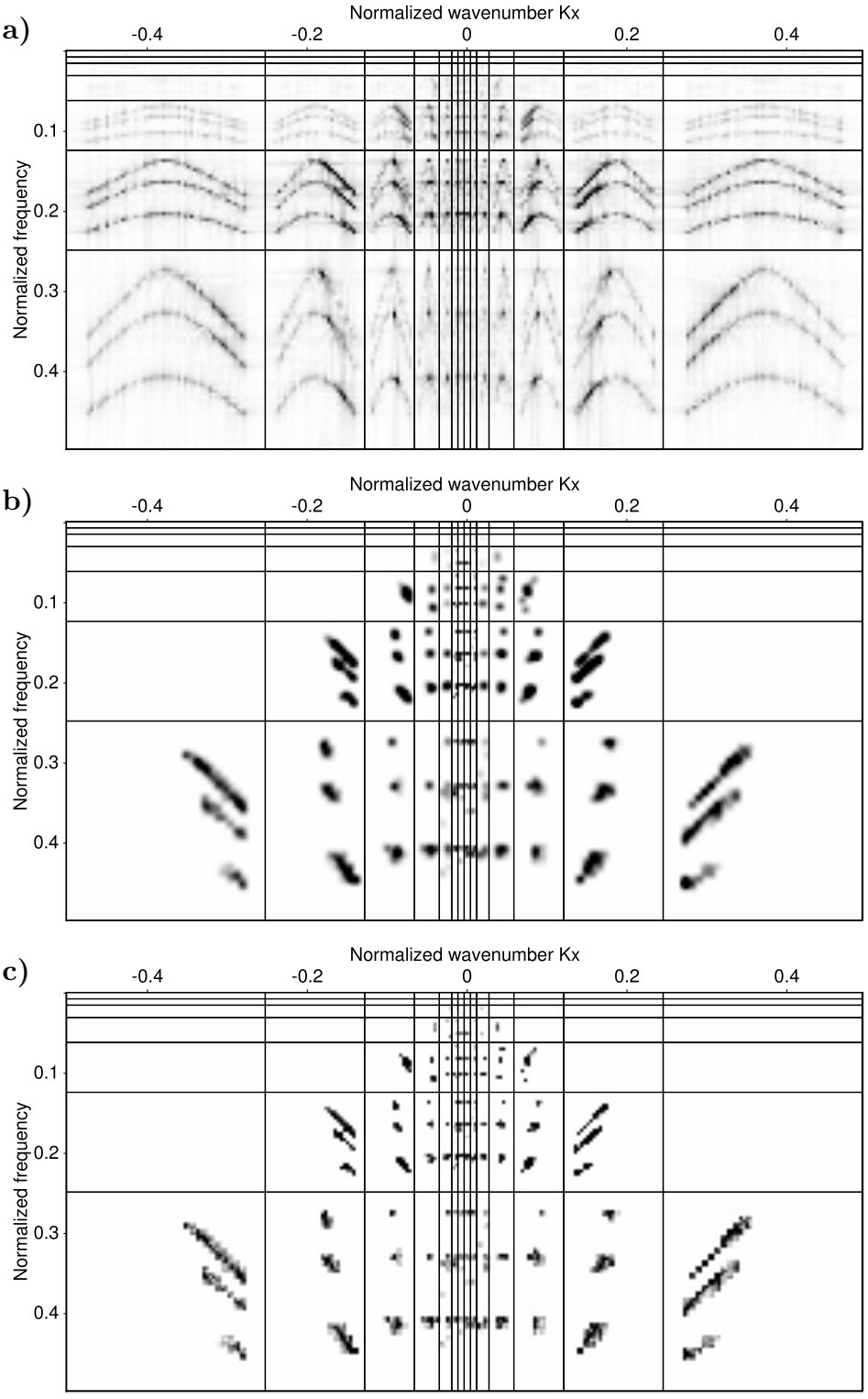

FIG. 6. a) 2D FGFT representation of data with missing traces in Figure 5a. b) Mask function built using Equations 12 and 13. c) 2D FGFT representation of interpolated data in Figure 5c.

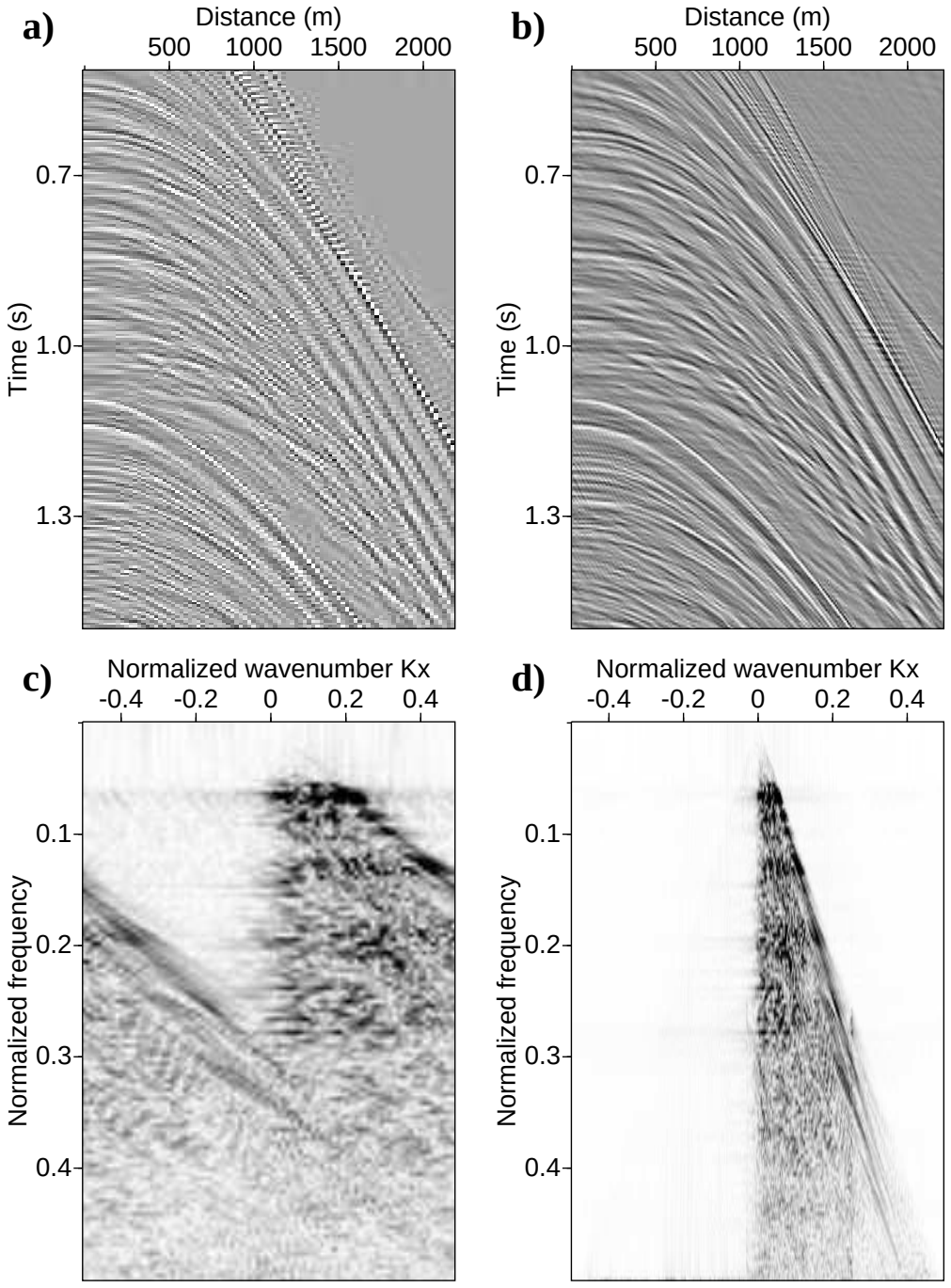

FIG. 7. a) Original shot recored from Gulf of Mexico data set. b) Interpolated data using 2D FGFT method. c) and d) are the *f-k* spectra of a and b, respectively

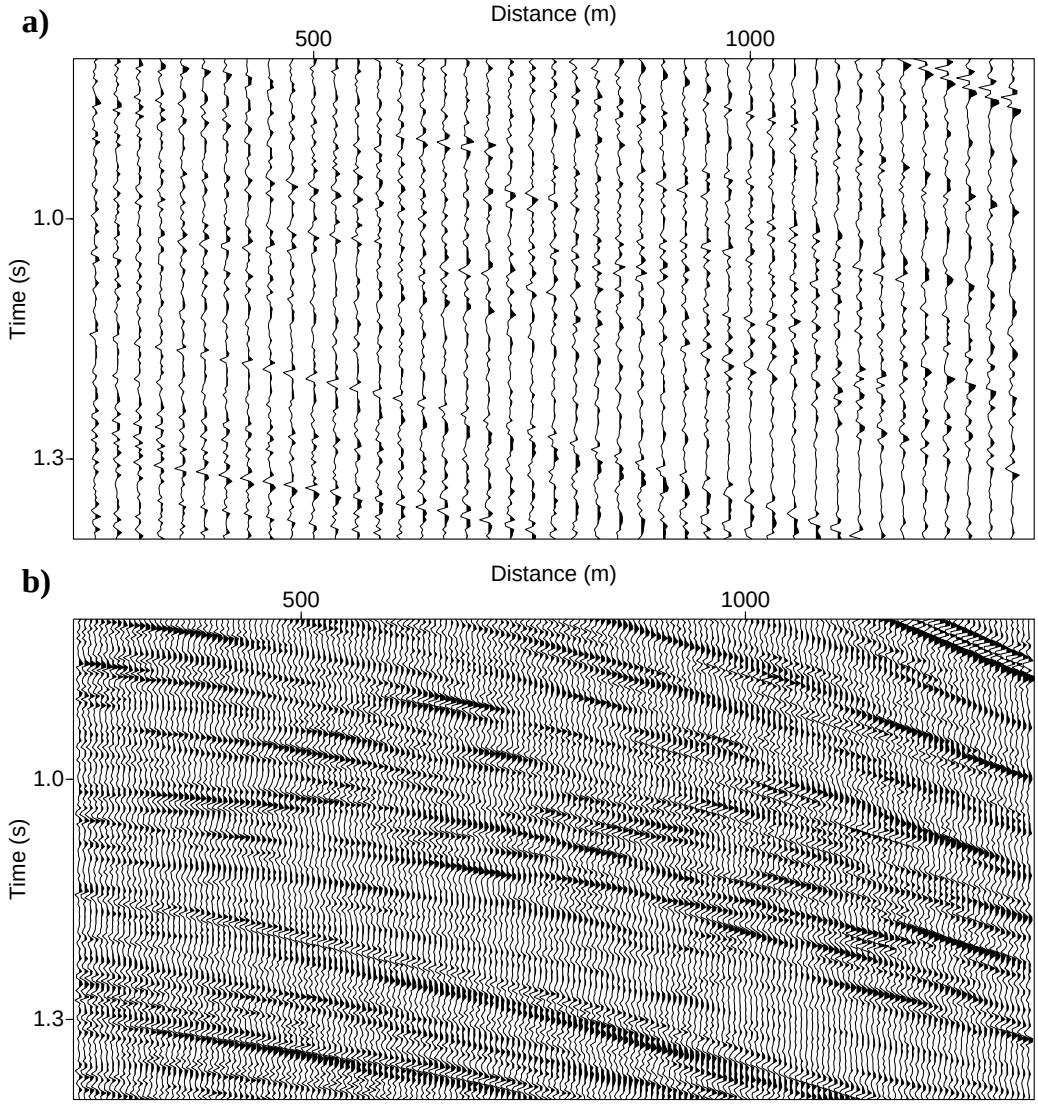

FIG. 8. a) A small window of original shot recored from Gulf of Mexico data set. b) Interpolated data using 2D FGFT method.

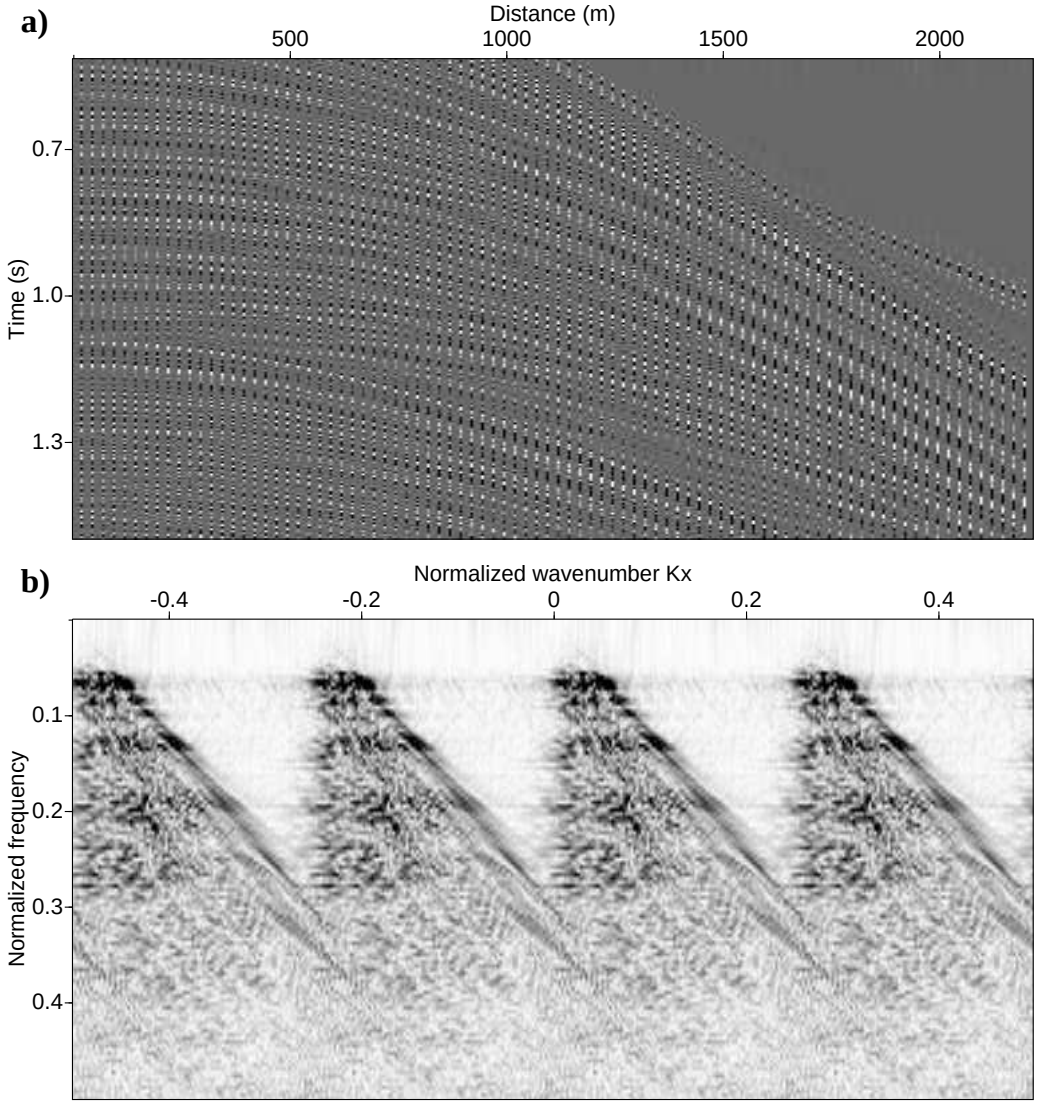

FIG. 9. a) Original shot record in Figure 7a after interlacing 3 zero traces between each pair of original traces. b) The *f-k* spectra of a.

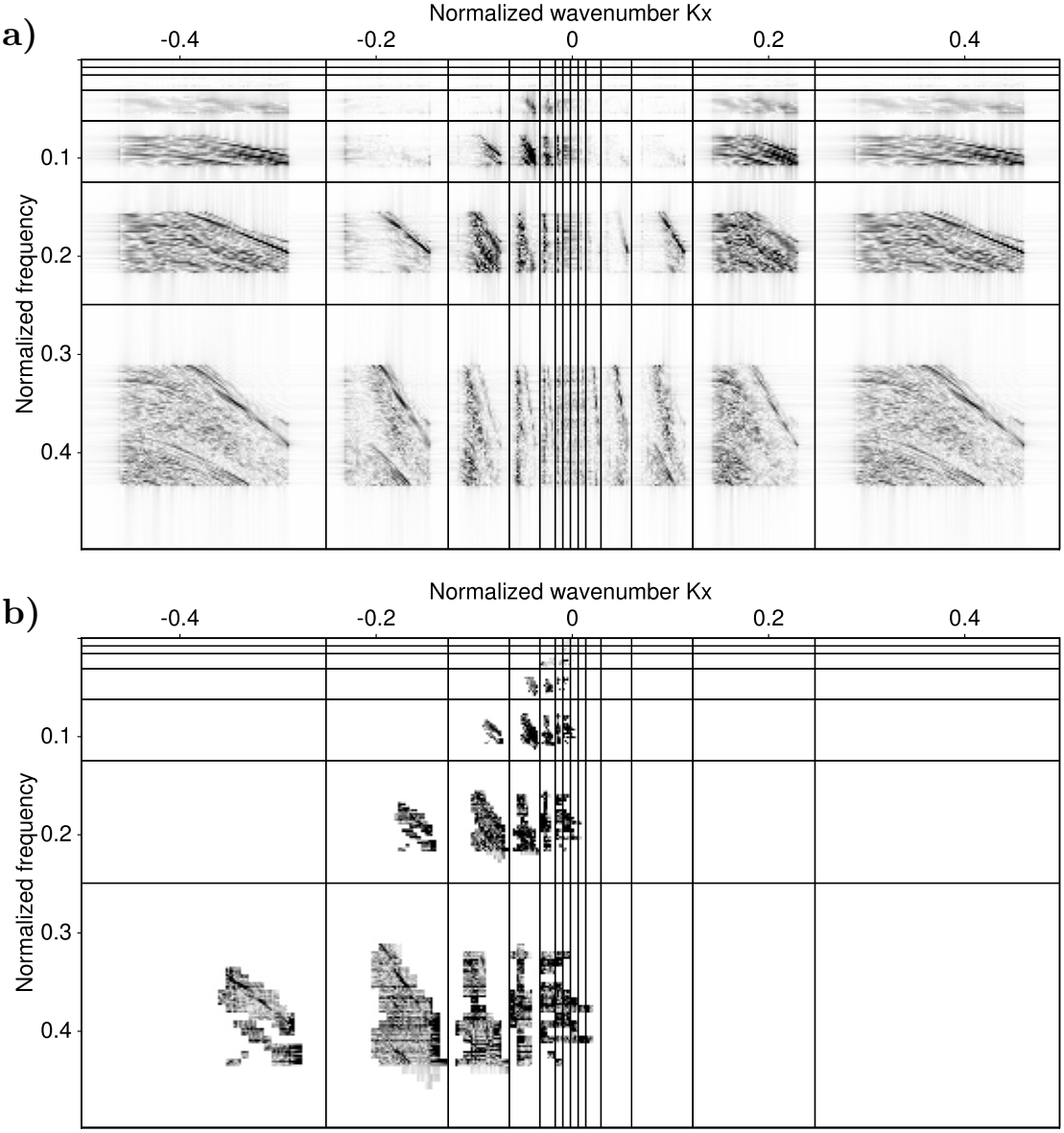

FIG. 10. a) 2D FGFT representation of data in Figure 9a. b) 2D FGFT representation of interpolated data in Figure 7b

padded region rather than wrapping-around and overlaying the desired part pf the data. The artifacts that appear in the zero-padded region of data can be easily truncated after interpolation. Also it is wise to smooth the weight function, in order to account for the uncertainties in the data thresholding process. One can also modify the 2D FGFT algorithm to gain more resolution by choosing overlapping tiles in the *f-k* domain with proper summation to unity weights in the corners. This can increase the computational cost of the algorithm, it might be necessary for some application which require high precision. For interpolation purposes the accuracy of ordinary 2D FGFT algorithm seems to be suficient.

CONCLUSIONS

We introduced and developed an interesting alternative for time-frequency and space-wavenumber analysis of 2D seismic signals with temporal and spatial dependencies. The 2D FGFT offers a fast and non-redundant algorithm to analyze 2D non-stationarity signals. It decomposes the seismic records based on the local slope information. This was effectively utilized for beyond-alias interpolation of the seismic record by projecting a weight function from alias-free low frequencies to alias-contaminated high frequencies. The integration of the latter with a least-squares fitting algorithm establishes a robust interpolation scheme for both regularly and irregularly sampled seismic records. Synthetic and real seismic data examples show the effectiveness of the 2D FGFT interpolation method.

ACKNOWLEDGEMENTS

We thank the financial support of the sponsors of the Consortium for Research in Elastic Wave Exploration Seismology (CREWES) at the University of Calgary.

REFERENCES

Abma, R., and Kabir, N., 2005, Comparison of interpolation algorithms: The Leading Edge, **24**, No. 10, 984–989.

Brown, R. A., Lauzon, M. L., and Frayne, R., 2010, A general description of linear time-frequency transforms and formulation of a fast, invertible transform that samples the continuous s-transform spectrum nonredundantly: IEEE Trans. Signal Processing, **58**, No. 1, 281–290.

Cadzow, J. A., and Ogino, K., 1981, Two-dimensional spectral estimation: IEEE Transactions on Acoustics, Speech, and Signal processing, **29**, No. 3, 396–401.

Candes, E. J., Demanet, L., Donoho, D. L., and Ying, L., 2005, Fast discrete curvelet transforms: Multiscale Modeling and Simulation, **5**, 861–899.

Claerbout, J., 1992, Earth Soundings Analysis: Processing Versus Inversion: Blackwell Science.

Curry, W., 2009, Interpolation with Fourier-radial adaptive thresholding: SEG, Expanded Abstracts, **29**, 3259 – 3263.

Duijndam, A. J. W., Schonewille, M. A., and Hindriks, C. O. H., 1999, Reconstruction of band-limited signals, irregularly sampled along one spatial direction: Geophysics, **64**, No. 2, 524–538.

Gibson, P. C., Lamoureux, M. P., and Margrave, G. F., 2006, Letter to the editor: Stockwell and wavelet transforms: The Journal of Fourier Analysis and Applications, **12**, No. 6, 713–721.

Guitton, A., and Claerbout, J., 2010, An algorithm for interpolation in the pyramid domain: Geophysical Prospecting, **58**, 965–975.

Gulunay, N., 2003, Seismic trace interpolation in the Fourier transform domain: Geophysics, **68**, No. 1, 355–369.

Hestenes, M. R., and Stiefel, E., 1952, Methods of conjugate gradients for solving linear systems: Journal of Research of the National Bureau of Standards, **49**, No. 6, 409–436.

Liu, B., and Sacchi, M. D., 2004, Minimum weighted norm interpolation of seismic records: Geophysics, **69**, No. 6, 1560–1568.

Menke, W., 1989, Geophysical Data Analysis: Discrete Inverse Theory: Academic Press.

Naghizadeh, M., 2010, A unified method for interpolation and de-noising of seismic records in the f-k domain: SEG Technical Program Expanded Abstracts, **29**, 3579–3583.

Naghizadeh, M., and Innanen, K. A., 2011, Seismic data interpolation using a fast generalized fourier transform: Geophysics, **76**, V1–V10.

Naghizadeh, M., and Sacchi, M. D., 2007, Multistep autoregressive reconstruction of seismic records: Geophysics, **72**, No. 6, V111–V118.

Naghizadeh, M., and Sacchi, M. D., 2009, *f-x* adaptive seismic-trace interpolation: Geophysics, **74**, No. 1, V9–V16.

Naghizadeh, M., and Sacchi, M. D., 2010a, Beyond alias hierarchical scale curvelet interpolation of regularly and irregularly sampled seismic data: Geophysics, **75**, No. 6, WB189–WB202.

Naghizadeh, M., and Sacchi, M. D., 2010b, On sampling functions and Fourier reconstruction methods: Geophysics, **75**, No. 6, WB137–WB151.

Oropeza, V., and Sacchi, M., 2011, Simultaneous seismic data denoising and reconstruction via multichannel singular spectrum analysis: Geophysics, **76**, No. 3, V25–V32.

Ozbek, A., Vassallo, M., Ozdemir, K., Van Manen, D., and Eggenberger, K., 2010, Crossline wavefield reconstruction from multicomponent streamer data: Part 2 - joint interpolation and 3d up/down separation by generalized matching pursuit: Geophysics, **75**, No. 6, WB69–WB85.

Ozdemir, K., Ozbek, A., Van Manen, D., and Vassallo, M., 2010, On data-independent multicomponent interpolators and the use of priors for optimal reconstruction and 3d up/down separation of pressure wavefields: Geophysics, **75**, No. 6, WB39–WB51.

Porsani, M., 1999, Seismic trace interpolation using half-step prediction filters: Geophysics, **64**, No. 5, 1461–1467.

Sacchi, M. D., Ulrych, T. J., and Walker, C. J., 1998, Interpolation and extrapolation using a high-resolution discrete Fourier transform: IEEE Transaction on Signal Processing, **46**, No. 1, 31–38.

Spitz, S., 1991, Seismic trace interpolation in the *F-X* domain: Geophysics, **56**, No. 6, 785–794.

Stockwell, R. G., Mansinha, L., and Lowe, R. P., 1996, Localization of the complex spectrum: The s transform: IEEE Trans. Signal Processing, **44**, No. 4, 998–1001.

Tikhonov, A. N., and Goncharsky, A. V., 1987, Ill-posed problems in the natural sciences: MIR Publisher.

Trickett, S. R., 2003, F-xy eigenimage noise suppression: Geophysics, **68**, No. 2, 751–759.

Trickett, S. R., and Burroughs, L., 2009, Prestack rank-reducing noise suppression: theory: SEG, Expanded Abstracts, **29**, 3332– 3336.

Vassallo, M., Ozbek, A., Ozdemir, K., and Eggenberger, K., 2010, Crossline wavefield reconstruction from multicomponent streamer data: Part 1 - multichannel interpolation by matching pursuit (mimap) using pressure and its crossline gradient: Geophysics, **75**, No. 6, WB53–WB67.

Xu, S., Zhang, Y., Pham, D., and Lambare, G., 2005, Antileakage Fourier transform for seismic data regularization: Geophysics, **70**, No. 4, V87–V95.